# KEAP1 inhibition is neuroprotective and suppresses the development of epilepsy

Shekh-Ahmad, Tawfeeq; Eckel, Ramona ; Dayalan Naidu, Sharadha; Higgins, Maureen; Yamamoto, Masayuki; Dinkova-Kostova, Albena

*Published in:*
Brain

*DOI:*
10.1093/brain/awy071

*Publication date:*
2018

*Document Version*
Peer reviewed version

This is a pre-copyedited, author-produced version of an article accepted for publication in Brain following peer review. The version of record Shekh-Ahmad, Tawfeeq et al."KEAP1 inhibition is neuroprotective and suppresses the development of epilepsy". Brain. 2018, 141(5). 1390-1403. Available: 10.1093/brain/awy071

# KEAP1 inhibition is neuroprotective and suppresses the development of epilepsy.

Tawfeeq Shekh-Ahmad[1], Ramona Eckel[1], Sharadha Dayalan Naidu[2], Maureen Higgins[2], Masayuki Yamamoto[3], Albena T. Dinkova-Kostova[2,4], Stjepana Kovac[1,5], Andrey Y. Abramov[1]*, Matthew C. Walker[1]*.

[1]UCL Institute of Neurology, University College London, Queen Square, London WC1N, UK
[2]Jacqui Wood Cancer Centre, Division of Cancer Research, School of Medicine, University of Dundee, Dundee, Scotland, United Kingdom
[3]Department of Medical Biochemistry, Tohoku University Graduate School of Medicine, Aoba-ku, Sendai, Japan
[4]Department of Pharmacology and Molecular Sciences and Department of Medicine, Johns Hopkins University School of Medicine, Baltimore, MD, USA
[5]Department of Neurology, University of Muenster, Muenster 48149, Germany

Correspondence to: Matthew C. Walker

UCL Institute of Neurology, Queen Square House, Queen Square, WC1N 3BG, London, UK

E-mail: m.walker@ucl.ac.uk

Correspondence may also be addressed to: Andrey Abramov

UCL Institute of Neurology, Queen Square House, Queen Square, WC1N 3BG, London, UKE-mail: (a.abramov@ucl.ac.uk)

Running title: KEAP1 inhibition and epileptogenesis

## Abstract

Hippocampal sclerosis is a common acquired disease that is a major cause of drug resistant epilepsy. A mechanism that has been proposed to lead from a brain insult to hippocampal sclerosis is the excessive generation of reactive oxygen species, and consequent mitochondrial failure.

Here we use a novel strategy to increase endogenous antioxidant defenses by using RTA 408, which we show activates nuclear factor erythroid 2-related factor 2 through inhibition of Kelch-like ECH associated protein 1 (Keap 1) through its primary sensor C151. Activation of nuclear factor erythroid 2-related factor 2 with RTA 408 inhibited reactive oxygen species production, mitochondrial depolarization and cell death in an *in vitro* model of seizure-like activity. RTA 408 given after status epilepticus *in vivo* increased ATP, prevented neuronal death, and dramatically reduced (by 94%) the frequency of late spontaneous seizures for at least four months following status epilepticus.

Thus, acute Keap1 inhibition following status epilepticus exerts a neuroprotective and disease modifying effect, supporting the hypothesis that reactive oxygen species generation is a key event in the development of epilepsy.

**Keywords**: Epilepsy, Epileptogenesis, Nrf2-KEAP1 pathway, oxidative stress, mitochondrial dysfunction

**Abbreviations:** ARE = antioxidant response elements; FCCP = carbonylcyanide-p-trifluoromethoxyphenyl hydrazine; GSH = Glutathione; HEt = dihydroethidium; HS = Hippocampal sclerosis; KA = Kainic acid; Keap1 = Kelch-like ECH associated protein 1; MCB = Monochlorobimane; NQO1 = NADPH:quinone oxidoreductase; Nrf2 = nuclear factor erythroid 2-related factor 2; ROS = reactive oxygen species ; SE = status epilepticus;

## Introduction

Epilepsy remains one of the commonest serious neurological diseases, affecting over 50 million people worldwide(de Boer *et al.*, 2008). This represents a considerable health care burden not just because of the impact of seizures, but also because of the increased morbidities and mortality associated with epilepsy. However, the medications that we presently have are designed to target the symptom, seizures, rather than modify the disease(Galanopoulou *et al.*, 2012). Many of the epilepsies are acquired conditions following an insult to the brain such as a prolonged seizure, traumatic brain injury or stroke, and an important challenge is to determine and treat the major pathways that lead from the insult to epilepsy (termed epileptogenesis)(Pitkanen and Lukasiuk, 2011). A number of potential strategies have been identified including targeting inflammation, disruption of the blood brain barrier, and gene expression with microRNAs(Vezzani *et al.*, 2011; Heinemann *et al.*, 2012; Reschke and Henshall, 2015). However, most of these treatments have modest effects or have only been shown to be effective if given during or before the insult (substantially lessening their translational potential).

A common sequela of brain injury is the generation of reactive oxygen species (ROS) and induction of oxidative stress. There is growing evidence that inhibiting ROS generation can ameliorate neuronal damage in seizures and epilepsy(Kim *et al.*, 2013; Kovac *et al.*, 2014; Williams *et al.*, 2015). However, the effects of antioxidant therapy on seizure development have been mixed. This may be partly explained by the short-lived neuroprotective effects of direct antioxidants, because of their consumption in the process of ROS scavenging. An alternative strategy is to increase the endogenous antioxidant defenses of cells by upregulating the transcription factor, nuclear factor erythroid 2-related factor 2 (Nrf2). Activation of Nrf2 has been shown to be protective against oxidative stress in a number of pathologies(Esteras *et al.*,

2016). In addition, activation of Nrf2 provides substrates for mitochondria and so increases ATP production, which can be protective for cells(Holmstrom *et al.*, 2013; Dinkova-Kostova and Abramov, 2015). Nrf2 has been shown to increase in kindled animals and after status epilepticus (SE) (Wang *et al.*, 2013), and overexpressing Nrf2 neuroprotects following SE (Mazzuferi *et al.*, 2013).

Sulforaphane, a naturally occurring Nrf2 activator, has therefore been proposed as a possible disease-modifying treatment in epilepsy(Pauletti *et al.*, 2017). However, sulforaphane is non-selective, affecting many off-target proteins(Clulow *et al.*, 2017), and can itself exhibit both anticonvulsant(Carrasco-Pozo *et al.*, 2015) and proconvulsant activity(Socala *et al.*, 2017). Moreover, sulforaphane is toxic at high dose, and has probable poor penetration of the blood brain barrier(Clarke *et al.*, 2011). Together, these may explain why a convincing effect on the development of seizures has only been shown when sulforaphane is administered with high dose antioxidants(Pauletti *et al.*, 2017).

In contrast to sulforaphane, cyanoenone triterpenoids are specific for Nrf2(Walsh *et al.*, 2014) and 200-400 times more potent than sulforaphane with a much higher therapeutic index(Copple *et al.*, 2014). One member of this chemical class, RTA 408, a close structural analog of bardoxolone methyl, is a novel Nrf2 activator that has undergone clinical trials in non-small cell lung cancer and, in part because of its CNS penetration properties, is now undergoing a clinical trial in Friedreich's Ataxia(SHEIKH, 2014). Here we show that RTA 408 activates Nrf2 through inhibition of Keap1 through its primary sensor C151. We further observed that RTA 408 inhibits ROS production, mitochondrial depolarization and cell death in an *in vitro* model of seizure-like activity. Importantly, our studies demonstrate that, given after SE *in vivo*, RTA 408 increases glutathione and ATP, and prevents neuronal death. Moreover, acute RTA 408 treatment alone

results in a dramatic reduction in spontaneous seizures for at least four months following SE. Acute inhibition of Keap1 by RTA 408 represents a novel approach to reduce neuronal death and modify the development of seizures.

## Materials and methods

### Cortical cell cultures

Mixed cortical neurons and glial cells cultures were prepared from postnatal (P0-P1) Sprague-Dawley rat pups (UCL breeding colony) according to a modified protocol described by Haynes(LW., 1999). The pups were sacrificed by cervical dislocation, and rat brains were quickly removed; neocortical tissue was isolated and submerged in ice-cold HBSS ($Ca^{2+}$, $Mg^{2+}$-free, ThermoFisherInvitrogen, Paisley, UK). The tissue was treated with 1% trypsin for 10 minutes at 37°C to dissociate cells. The final neuronal cell suspension was plated on 25 mm round coverslips coated with poly-L-lysine (1 mg/ml, Sigma), and cultured in Neurobasal A medium supplemented with B-27 (ThermoFisherInvitrogen) and 2 mM L-glutamine.

Neocortical cultures were fed once a week and maintained in a humidified atmosphere of 5% $CO_2$ and 95% air at 37 °C in a tissue culture incubator.

The cultures were used for experiments at 13-17 days *in vitro* (DIV). Neurons were distinguished from glia by their typical appearance using phase-contrast imaging.

### Recording solutions

Preincubations and experiments were performed at room temperature (RT), unless otherwise mentioned, and were performed in an HEPES-buffered salt solution (aCSF), composition (in mM): 125 NaCl, 2.5 KCl, 2 $MgCl_2$, 1.25 $KH_2PO_4$, 2 $CaCl_2$, 30 glucose and 25 HEPES, pH adjusted to 7.4 with NaOH.

Experiments were carried out in the HEPES buffered salt solution including (aCSF) or excluding $MgCl_2$ (low-$Mg^{2+}$) to induce seizure-like activity.

## Imaging of intracellular $Ca^{2+}$ ($[Ca^{2+}]c$) and mitochondrial membrane potential ($\Delta\psi m$)

Before recording, neocortical neuronal cultures were incubated for 30 minutes with 5 μM Fura-2-AM (ThermoFisher-Invitrogen, Paisley, UK), and 0.005% pluronic acid in aCSF.

For simultaneous measurement of $[Ca^{2+}]_c$ and $\Delta\psi m$, Rhodamine123 (Rh123) (Sigma, UK) (1 μM) was added into the culture dishes during the last 15 minutes of the Fura-2-AM loading period. Cells were then washed 3 times prior to recordings. $[Ca^{2+}]_c$ was expressed by the Fura-2 ratio. An increase of Rh123 signal indicates depolarization of mitochondria. Rh123 signals were normalized to the baseline level (set 0) and maximum signal produced by mitochondrial oxidative phosphorylation uncoupling with carbonylcyanide-p-trifluoromethoxyphenyl hydrazone (FCCP, 1 μM; set to 100). Cells were then washed 3 times prior to recordings. Seizure activity was induced by excluding $MgCl_2$ from the medium.

Experiments were repeated at 5-7 times with > 3 different cultures.

## Imaging of intracellular ROS generation

To evaluate rates of ROS production in the cytosol, dihydroethidium (HEt; 5 μM) was present in all solutions throughout the experiments. No pre-incubation was used to avoid accumulation of oxidized products. Experiments were conducted using 2-3 separate cultures and repeated on 4-6 coverslips.

## Imaging of Glutathione (GSH)

For GSH measurements, the media was replaced with either aCSF or low-$Mg^{2+}$ aCSF and cells were incubated with 50 μM Monochlorobimane (MCB) (Sigma, St. Louis, MO) for 1 h at room temperature. The cells were then washed with aCSF, and images of the fluorescence of the MCB-GSH adduct were acquired using a cooled CCD imaging system. Experiments were repeated on 9-10 coverslips using > 3 separate cultures.

## Neuronal death

Neurotoxicity was determined following incubation with low-$Mg^{2+}$ for 2 h at 37 °C, by co-staining cells with propidium iodide (20 μM) and Hoechst 33342 (4.5 μM) (Sigma, St. Louis, MO) in a fluorescent live/dead assay. Experiments were conducted on 3 separate cortical cultures and repeated on 9 coverslips for each treatment. In each treated culture coverslip, 5 random fields were counted.

## Live imaging and analysis

Fluorescence images were obtained on an epifluorescence inverted microscope with a 20× fluorite objective. Excitation light provided by a xenon arc lamp, the beam passing monochromator at 340, 380, 490 or 530 nm (HEt) (Cairn Research, Kent, UK). Emitted fluorescence was detected by a cooled CCD camera (Retiga; QImaging).

$[Ca^{2+}]_c$ and mitochondrial membrane potential were measured in single cells and traces are presented as the ratio of excitation at 340 and 380 nm, both with emission at 515 nm. An increase of Rhodamine123 signal indicates depolarisation of mitochondria. Rhodamine123 signals were normalised to the baseline level (set 0) and maximum signal produced by mitochondrial oxidative phosphorylation uncoupling with carbonylcyanide-p-trifluoromethoxyphenyl hydrazone (FCCP, 1 μM; set to 100). Phototoxicity and photobleaching of cells was minimized by limiting light exposure to the time of acquisition of the images. Fluorescent images were acquired with a frame interval of 10 s. Data were analyzed using Andor software (Belfast, UK).

HEt was excited by illumination at 530 nm. For most of the experiments, we chose to perform measurements of ROS production rates with HEt at a single wavelength, first to avoid photobleaching and phototoxicity from excitation of cells in the range of UV light. Rates of ROS increase were calculated at different time points (2, 10 and 15 min) after exposure to low-$Mg^{2+}$ and were compared with rates recorded during a 1-3 min aCSF exposure period referred to as baseline.

Images of the fluorescence of the MCB-GSH adduct were acquired using a cooled CCD imaging system as described using excitation at 380 nm and emission at 400 nm.

In all the experiments, each culture coverslip represents the average of 70-120 neurons.

## NQO1 Bioassay

Hepa1c1c7 murine hepatoma cells were grown in α-MEM supplemented with heat- and charcoal-treated 10% (v/v) fetal bovine serum. Mouse embryonic fibroblasts isolated from WT or Nrf2-KO mice were grown in in Iscoves Modified Dulbecco's Medium (with L-glutamine), supplemented with 10% (v/v) heat-inactivated fetal bovine serum, 1 x insulin-transferrin-selenium, and 10 ng/ml epidermal growth factor (Gibco-Invitrogen, Paisley, UK)(Higgins and Hayes, 2011). Cultured cells were maintained in a humidified atmosphere at 37°C, 5% $CO_2$. For evaluation of the NQO1 inducer activity, cells ($10^4$ per well) were grown for 24 h in 96-well plates. The medium was then replaced with RTA 408-containing fresh medium, and the cells were further grown for either 48 h (Hepa1c1c7) or 24 h (MEFs). There were eight replicates of each treatment of eight different concentrations of the inducer. RTA 408 was dissolved in acetonitrile, and diluted in the cell culture medium at a ratio of 1:1000. The final acetonitrile concentration in the medium was 0.1% (v/v) in all wells. At the end of the treatment period, cell lysates were prepared in digitonin and the specific activity of NQO1 was determined using menadione as a substrate as described(Fahey *et al.*, 2004).

## Generation of stable Keap1-rescued MEF cell lines and Keap1$^{C151S/C151S}$ knock-in mice

All mouse experiments were performed according to the regulations of The Standards for Human Care and Use of Laboratory Animals of Tohoku University (Sendai, Japan) and the Guidelines for Proper Conduct of Animal Experiments of the Ministry of Education, Culture, Sports,

Science, and Technology of Japan. Immortalized Keap1-knockout (KKO) MEF cells were grown in low glucose Dulbecco modified Eagle medium (Wako Chemical, Japan) supplemented with 9% (v/v) fetal bovine serum at 37°C and 5% $CO_2$. The PiggyBac transposon system (PB514B-2; System Biosciences, California, USA) was utilized to generate stable cell lines expressing HA-tagged mouse Keap1 (HA-Keap1) or cysteine mutants of HA-Keap1 as described(Saito *et al.*, 2015). *Keap1*$^{C151S/C151S}$ knock-in mice were generated using the CRISPR/Cas9 technology(Saito *et al.*, 2015). Thioglycollate-elicited peritoneal macrophages were collected by lavage from *Keap1*$^{C151S/C151S}$ knock-in mice and their WT counterparts. The primary peritoneal macrophage cells were grown at 37°C and 5% $CO_2$ in RPMI 1640 medium supplemented with 10% (v/v) fetal bovine serum and penicillin-streptomycin (10 U/0.1 mg/ml).

## Immunoblotting

For immunoblotting analysis, cells were grown for 24 h in 6-well plates, and then treated with RTA 408 for a further 3 h. Cells were then washed with PBS, and lysed in 200 μl of lysis buffer [100 mM Tris-HCl, pH 6.8; 4% (w/v) sodium dodecyl sulfate (SDS); 20% (v/v) glycerol; 0.001% (w/v) Bromophenol Blue]. The cell lysates were subjected to sonication for 30 seconds, and then heated at 95°C for 5 min. After cooling, dithiothreitol (DTT) was added to a final concentration of 20 mM, and the lysates were incubated at 37°C for 10 min. Protein concentrations were determined by the BCA assay (Thermo Fisher Scientific, Waltham, (Massachusetts, USA. Proteins (15-20 μg) were resolved by electrophoresis on an 8% SDS–polyacrylamide gel, and electrophoretically transferred to a polyvinylidene difluoride (PVDF) membrane. After blocking with 10% non-fat milk at room temperature for 1 h, immunoblotting was performed with the following antibodies and dilutions: rat monoclonal Nrf2 antibody(Saito

*et al.*, 2015) (1:100), rat monoclonal HA antibody (Roche, 3F10, California, USA, 1:1000), rat monoclonal Keap1 antibody(Saito *et al.*, 2015) (1:100), and mouse monoclonal α-tubulin antibody (Sigma–Aldrich, DM1A, 1:5000-1:10000 dilution). The western blot data are representative of three independent experiments.

## Animals

Animal experiments were conducted in accordance with the Animals (Scientific Procedures) Act 1986, and approved by the local ethics committee. Male Sprague-Dawley rats (Charles River Laboratories, UK; 160-180 g) were individually housed with free access to food and water in 12 h light/dark cycles throughout the study. Animals were acclimatised to the animal house for at least 7 days before experimental use. There was no difference in weight between the animals randomised to vehicle or RTA 408 (248±8 vs. 257±9 grams, respectively).

## Surgery

Male Sprague–Dawley rats were anaesthetized using isoflurane and placed in a sterotaxic frame (Kopf, CA, USA). At the start of surgery, Buprenorphine (0.2 mg/kg; SC) and Metacam (1 mg/kg; SC) were administered for pain relief. An EEG transmitter (A3028, Open Source Instruments)(Chang *et al.*, 2011) was implanted subcutaneously. A subdural intracranial recording electrode was positioned above the right hippocampus (2.5 mm lateral and 4 mm posterior of bregma(Paxinos G., 1998)), and a reference electrode was implanted in the contralateral hemisphere (2.5 mm lateral and 6 mm posterior of bregma). The electrodes were fixed to the skull with three skull screws and tissue glue, followed by dental cement.

Immediately after surgery, 3-5 ml of warmed Ringer's solution and Amoxicillin (Betamox LA, 100 mg/kg) was administered subcutaneously. Rats recovered for 7-10 days before initiation of the experiment. Rats were housed separately in Faraday cages and EEG was recorded continuously for up to 18 weeks post-surgery.

## KA induced SE epilepsy model

For induction of SE, kainic acid (KA) treatment was used according to a protocol described by Hellier et al(Hellier *et al.*, 1998). This model has a low mortality rate and reliably leads to later spontaneous recurrent seizures(Williams *et al.*, 2009; Jupp *et al.*, 2012; Liu *et al.*, 2016). Rats were injected intraperitoneally with KA (Tocris Bioscience, Bristol, UK) dissolved in sterile 0.9% saline (10 mg/mL) at a dose of 5 mg/kg. Rats were continuously monitored for convulsive motor seizures and for EEG in those rats with implanted transmitters. Hourly KA treatment continued in animals without convulsive seizures until class III, IV, or V seizures were evoked (scored according to a modified Racine's scale(Racine, 1972; Ben-Ari, 1985)). Once an animal began showing excessive inactivity or excessive activity (i.e. exaggerated running or jumping), or had more than 10 class IV/V seizures/h, subsequent injections were delayed or reduced to 2.5 mg/kg to avoid excessive toxicity and mortality. The endpoint for KA treatment was considered either when animals reached class V seizure (i.e. excessive rearing with concomitant forelimb clonus and falling) or when the total dose of KA reached 45 mg/kg.

Animals were included in the study if there was continuous epileptiform activity for 2 h, during which spike frequencies were more than 2 Hz, and spike amplitude was at least 3 times background. For rats that were not EEG monitored, duration of SE was measured based on behavioral manifestation. Start of the status was considered when the rat experienced full motor

seizure with loss of postural control and falling. The SE was terminated in all animals at 2 hours by intraperitoneal administration of diazepam (5mg/kg ip). All animals were randomized to treatment group prior to SE to prevent any bias in length of SE or number of doses of KA.

## Drugs administration

Following 2 h of SE, rats were randomized to treatment with either vehicle (10% DMSO/sterile saline) or RTA 408 dissolved in the same vehicle. RTA 408 was synthesized by Reata Pharmaceuticals, Inc. In multiple dose experiments, control animals were treated with an equivalent volume and number of injections of vehicle as the RTA 408 treated animals.

## EEG analysis

The seizure detection analysis was performed in an automated manner with custom-written software to minimize the potential for bias. EEG was processed with the Neuroarchiver tool (Open Source Instruments), which determined EEG power for different frequency bands. Seizures were characterized by the appearance of high frequency (>2 Hz) with progression of the spike frequency, rhythmic spike wave discharges with amplitudes at least three times that of baseline EEG (see Fig. 5b) that lasted for a minimum of 10 s. All electrographic seizures were confirmed by visual inspection. The majority of seizures were confirmed by video monitoring.

## Video monitoring

Out of 18 rats recorded for EEG used in this study, 14 rats were simultaneously video monitored 24 h/d throughout the study with video IP cameras. The time stamps for cameras were synchronized to the EEG digitizing computer. Cameras were placed 30-40 cm from each rat. The behavioral data were used in this study in cases where EEG seizure activity needed to be distinguished from electrical noise generated by movement artifacts.

### *in vivo* Glutathione measurements

Total (oxidized and reduced forms) Glutathione concentrations were determined by Glutathione Assay Kit (Cat No. CS0260, Sigma). The brain tissue was collected from sham rats (Sham, n = 7 for cortex and n = 6 for hippocampus) and from treated rats 7 days following KA-induced SE for 2 h, followed by treatment with vehicle (10% DMSO/Saline, KA + vehicle; n = 5), RTA 408 groups at doses: 17.5 mg/kg once daily for 3 days (KA + RTA 17.5; n = 6), 25mg/kg once daily for 3 days (KA + RTA 25; n = 5) and 50mg/kg once daily for 2 days (KA + RTA 50; n = 6). Immediately following dissection, tissue was flash frozen by immediate immersion in liquid nitrogen. Tissue (200 mg of lateral part of frontal cortex and 50 mg of dorsal hippocampus) then was homogenized in 5 % SSA solution. After centrifuging at 10,000×g for 10 min, 10 µL supernatant was used for reaction with 150 µL working mixture (glutathione reductase and DTNB solution) at room temperature for 5 min. After that 50 µL nicotinamide adenine dinucleotide phosphate (NADPH) solutions were added to initiate the reaction. The glutathione content was determined by kinetic measurement with 1 min intervals for 5 min at 412 nm and calculated by comparison with standards. For the analysis, investigators were blinded to treatment.

## *in vivo* ATP measurements

ATP was measured in rat brain (cortex and hippocampus) using ATP-luciferase-based bioluminescence assay kit (Lonza, Basel, Switzerland). The brain tissue was collected from sham rats (Sham, n = 6) and from treated rats 7 days following KA-induced SE for 2 h, followed by treatment with vehicle (10% DMSO/Saline, KA + vehicle; n = 5), RTA 408 groups at doses: 17.5 mg/kg once daily for 3 days (KA + RTA 17.5; n = 5), 25mg/kg once daily for 3 days (KA + RTA 25; n = 5) and 50mg/kg once daily for 2 days (KA + RTA 50; n = 6). Briefly, immediately following dissection, tissue was flash frozen by immediate immersion in liquid nitrogen. Tissue (50 mg) was lysed in 500 µl of lysis reagent (for 10 min at room RT) and centrifuged at 10,000 × g for 2 minutes to pellet insoluble materials. To 100µl of resulting supernatant, 100 µl of ATP monitoring reagent was added in a 96-well plate. After 2 min incubation, luminescence was measured using Fluostar Omega microplate reader. ATP standard curve was created, and ATP concentration in the tissue lysed from animals was calculated relative to the standard curve, and expressed in nmols/g tissue. Analysis was performed blinded to treatment.

## Immunohistochemistry

One week or 15 weeks post KA-induced SE, rats were perfused transcardially under terminal anesthesia (Pentobarbital sodium) with heparinized phosphate-buffered saline (PBS; 8 IU/ml), followed by 4% paraformaldehyde (PFA) in PBS (Santa Cruz Biotechnology, Santa Cruz, CA, USA). Brains were removed and left in 4% PFA/PBS overnight at 4°C, and then cryoprotected with a 10-20-30% sucrose PBS gradient over 3-4 days until tissue sinks. After cryoprotection, brains were embedded in OCT Compound (Sakura Finetek, CA, USA) and

stored at -80 °C. For each animal, coronal sections (50 μm) selected from bregma -3.1 to 4 mm were cut in a cryostat (Leica CM1950) at -20C and fixed on poly-L-lysine coated slides (Thermo Fisher Scientific), then left to air dry at RT for 2 h. Brian sections were then circled with a water repellent pen (Dako pen; Agilent, CA, USA), permeabilized with PBS, 0.3% Triton X-100 for 30 min, blocked with 4% goat serum (Sigma) for 1 h and washed three times for 10 min each with PBS. Sections were incubated overnight at 4 °C with a rabbit primary antibody against NeuN (1:1000, MAB377, Millipore) in a solution of PBS and 0.3% Triton X-100. Following three washes with PBS (10 min each), the sections were incubated with Alexa fluor-488 goat anti mouse secondary antibody (1:1000; Abcam) for 2 h at RT. The sections were washed three times with PBS (10 min each) and mounted with Vectashield and 4',6-diamidino-2-phenylindole (DAPI) mounting medium (Vector Labs). In some sections, we also immunostained for the astrocytic marker glial fibrillary acidic protein (GFAP; Sigma, 1:400) followed by secondary antibody (Alexa fluor 594, Invitrogen). Images were obtained at a resolution of 1024 × 1024 on Zeiss confocal microscope using 20× objective. Images were acquired at 405 nm excitation wavelength and 455nm emission wavelength for DAPI; at excitation of 488 nm and emission of 510-613 nm for NeuN; and at excitation of 591 nm and emission of 605-652 nm wavelength for GFAP. Image analysis was performed using ImageJ software in an automatic cell counting image-based tool, and investigators were blinded to treatment. Neurons were identified as NeuN-positive cells with relatively large (>8 μm) soma. Cell densities for individual animals represent the average densities of the particular region for 4-6 brain sections. Results are expressed as neurons (or astrocytes) per $mm^2$. We quantified neuronal damage in the dorsal and ventral hippocampus, and we focused on the hippocampus as this is the brain area in which there is the greatest atrophy in this model as measured by

volumetric MRI(Jupp *et al.*, 2012). The cell counts were performed in the pyramidal cell/dentate granule cell layers where the predominant cell types are excitatory neurons.

### Statistical analysis.

Data are expressed as the mean ± SEM. Data were analyzed using unpaired Student's t test, Mann-Whitney U test, one-way ANOVA with Bonferroni *post hoc* test, or one-way repeated measures ANOVA with sequential Bonferroni *post hoc* test, as appropriate using SPSS 22 (IBM). The comparison of seizure frequency was analyzed using a generalized log-linear mixed model with random effect of animal (autoregressive covariance) and fixed effects of treatment group, week, and the interaction between treatment group and week. Sample sizes were chosen based on our previous experiences in the calculation of experimental variability. The numbers of animals used are described in the corresponding figure legends.

## Results

### RTA 408 activates Nrf2 by inhibition of its main negative regulator, Keap1

Using a Hepa1c1c7 murine hepatoma cell culture, we first tested whether the pentacyclic cyanoenone triterpenoid RTA 408 (Fig. 1a) induced the prototypic Nrf2 target enzyme NQO1, and demonstrated that it did so with a CD (Concentration that Doubles the specific activity of NQO1) of 2.5 nM (Fig. 1b) and that its ability to induce NQO1 was lost in the absence of Nrf2 (Fig. 1c).

Induction of Nrf2 is predominantly triggered by inactivation of Keap1, the mammalian cysteine-based sensor for electrophiles and oxidants (Dinkova-Kostova *et al.*, 2017). Chemical modification(s) of the cysteine sensor(s) of Keap1 inactivate its substrate adaptor function, leading to Nrf2 stabilization and subsequent upregulation of Nrf2-dependent transcription. We therefore next sought to identify the cysteine sensor(s) within Keap1 for RTA 408(Cleasby *et al.*, 2014; Huerta *et al.*, 2016). We used Keap1 knockout (KKO) mouse embryonic fibroblast (MEF) cells rescued with N-terminally hemagglutinin (HA)-tagged murine Keap1 ligated to the PiggyBac transposon system(Saito *et al.*, 2015). Expression plasmids encoding wild-type (WT) or cysteine mutants of three different types (i.e. C151S, C273E/C288W and C151S/C273W/C288W) HA-Keap1 were transfected into KKO MEF cells, and stable HA-Keap1 expressing lines were established.

We found that upon a 3-h exposure to 25 nM or 50 nM RTA 408, Nrf2 is stabilized in the WT and in the double mutant C273W/C288E Keap1-rescued KKO MEF cells (WT-KKO MEFs and C273W/C288E-KKO MEFs respectively) (Fig. 1d). By contrast, in the single mutant C151S Keap1-rescued KKO MEFs (C151S-KKO MEFs) and the triple mutant C151S/C273W/C288W Keap1-rescued KKO MEF cells (C151S/C273W/C288W-KKO MEFs), these concentrations of RTA 408 were unable to cause stabilization of Nrf2 (Fig. 1d). Furthermore, we used primary peritoneal macrophage cells isolated from WT or Keap1$^{C151S/C151S}$ knock-in mice that were generated using the CRISPR/Cas9 technology(Saito *et al.*, 2015). In agreement to the results obtained in Fig 1d, exposure of these cells to 15 nM or 30 nM RTA 408 for 3-h led to Nrf2 stabilization only in the WT, but not in the Keap1$^{C151S/C151S}$ primary peritoneal macrophage cells

(Fig. 1e). Taken together, these results establish that C151 in Keap1 is the primary sensor for RTA 408.

## RTA 408 prevents mitochondrial depolarization without altering calcium oscillations during epileptiform activity

We next determined the functional effect of Keap1 inhibition by RTA 408 in an *in vitro* model of epileptiform activity. We induced epileptiform activity through removal of magnesium from the medium; this promotes NMDA receptor activation by vesicular glutamate release and results in seizure-like activity and calcium oscillations in neurons(Kovac *et al.*, 2012). The omission of magnesium from the solution induced synchronised calcium signals in the control neuronal culture (Fig. 2a, n = 70 neurons, 1 experiment (exp.)). Pre-incubation (24 hours) of the cells with 200 nM RTA 408 did not change the frequency or coastline of low magnesium-induced calcium spikes in neuronal culture (Fig. 2 b-d). These data suggest that activation of Nrf2 with 200 nM RTA 408 did not change vesicular glutamate release or activation of NMDA receptors in the low magnesium model.

Prolonged seizure-like activity in neurons leads to mitochondrial depolarization, which may be the result of a low level of mitochondrial substrates, and/or opening of the mitochondrial permeability transition pore(Schuchmann *et al.*, 1999; Kovac *et al.*, 2012). Omission of magnesium from the recording medium induced slow and progressive mitochondrial depolarization in primary neurons resulting in ~30 % decrease in mitochondrial membrane potential ($\Delta\psi m$) in 30 min (Fig. 2e). Pre-incubation of the cells with 200 nM RTA 408 for 24 hours protected neurons against a decrease $\Delta\psi m$ (Fig. 2e).

Importantly, incubation of cells with a lower concentration of RTA 408 (50 nM) also effectively reduced the effect of low magnesium on mitochondrial membrane potential (Fig. 2e). Thus, activation of Nrf2 by incubation with RTA 408 supports mitochondrial metabolism that makes neuronal mitochondria less vulnerable to seizure-like activity.

## RTA 408 reduces epileptiform activity-induced ROS production and protects neurons against oxidative stress and excitotoxicity

In agreement with previously published studies(Kovac *et al.*, 2014; Williams *et al.*, 2015), we found that activation of epileptiform activity by omitting magnesium from the medium induced more than a 5-fold increase in the rate of ROS production (n = 403 neurons, 5 exp., Fig. 2f). Incubation of co-culture of neurons and astrocytes with 200 nM RTA 408 for 24 hours significantly reduced the rate of ROS production in neurons during seizure-like activity 2, 10 and 15 min after exposure to low-$Mg^{2+}$ (from 192%, 357% and 564% to 113%, 186 and 291% respectively, $F(2,12) = 49.415$, $p < 0.001$, Fig. 2f). There was no difference in ROS production between RTA 408 pre-treated neurons and low $Mg^{2+}$ condition at all time points (2 and 10 min: $p = 1.000$; 15 min: $p = 0.107$).

Generation of ROS in brain cells has physiological roles(Angelova and Abramov, 2016) and it becomes pathological only when it starts to reduce cellular antioxidants. Epileptiform activity significantly decreases the level of the major endogenous antioxidant in the central nervous system, glutathione (GSH; Fig. 2g), which indicates oxidative stress. Preincubation (for 24 hours) of the cortical neurons and astrocytes with 200 nM RTA 408 completely restored the GSH pool in cells with seizure-like activity (Fig. 2g).

We subsequently determined if this reduction of ROS production translated to a neuroprotective effect. Incubation of the cortical primary co-cultures of neurons and astrocytes in low magnesium medium for 2 hours induced neuronal loss (32% ± 2.4; Fig. 2h). Activation of Nrf2 by a 24-h preincubation of the cells with RTA 408 (200 nM) almost completely prevents seizure-like activity induced neuronal cell death (Fig. 2h).

## RTA 408 increases glutathione and ATP and prevents neuronal death following status epilepticus *in vivo*

We next asked if the antioxidant effects of RTA 408 observed *in vitro* translate to increased glutathione and ATP *in vivo*. We induced SE using KA, and the animals were randomised to either vehicle once a day for three days, or RTA 408 either as three dosing regimens: 17.5 mg/kg or 25 mg/kg over three days, or 50 mg/kg for two days. Although glutathione levels drop immediately following SE(Cock *et al.*, 2002), we found that in our SE model, they are normal by one week (Fig. 3a). However, in the RTA 408 treated SE animals, there was a significant dose-dependent increase in glutathione to supra-normal levels by one week post-SE (Fig. 3a). This was particularly evident in the hippocampus, which at the higher RTA 408 doses demonstrated a 3-4 fold increase in glutathione levels (Fig. 3a). Moreover, at one week post-SE, ATP levels were reduced in the vehicle treated animals but were restored to supranormal levels in a dose dependent fashion by RTA 408 (Fig. 3b). Since 25 mg/kg RTA 408 was well tolerated and restored the ATP levels at one week (Fig. 3b), and 50 mg/kg RTA 408 was associated with adverse effects (mainly weight loss) in subsequent experiments we used 25mg/kg RTA 408 as either a single dose or 3 doses over 3 days.

Is this increase in glutathione and protection against ATP depletion associated with neuroprotection? KA-induced SE results in significant neuronal damage in the hippocampus that can continue to progress for up to 8 weeks(Hopkins *et al.*, 2000; Jupp *et al.*, 2012). We, therefore, measured cell densities in the hippocampal subfields of the dorsal hippocampus one week and 15 weeks after SE. Significant neuronal loss in the hilus and CA3 is evident at 1 week post-SE (Fig. 4c,d) and does not progress by 15 weeks (Fig. 4a,f,g) . This loss was significantly ameliorated by RTA 408 (Fig. 4 a,c,d,f,g). There was only a non-significant trend for decreased neuronal densities in CA1 at one week (Fig. 4b); however, at 15 weeks there had been progressive CA1 neuronal loss, resulting in a significant decrease in neuronal density ($p < 0.001$ by unpaired two-tailed Student t-test, Fig. 4a,e). RTA 408 prevented this progressive neuronal loss in CA1 in a dose dependent fashion (Fig. 4a,e). We also analysed the effects of RTA408 on neuronal and glial damage in the ventral hippocampus at 15 weeks (Supplementary Figure 1) and found a similar degree of damage and protective effect in CA1 and CA3 (Supplementary Fig 2).

## RTA 408 modifies seizure progression

Although neuronal loss in the hippocampus is associated with cognitive and neurological deficits following SE, decreasing neuronal loss does not necessarily affect the development of epilepsy(Khalil *et al.*, 2017). We therefore separately tested if RTA 408 given after SE could prevent the development of epilepsy. Animals were randomly assigned to treatment with vehicle or RTA 408. Seizures were recorded in 9 animals (per group) for 12 weeks, and in 4 out of 9 animals in each group recordings were continued to 15 weeks.

All animals had SE lasting at least 2 hours, terminated with diazepam (5mg/kg ip) (Fig. 5a). Following SE, the rats developed spontaneous seizures (Fig. 5b). There was no significant

difference between the two groups in terms of total dose of KA (vehicle 16 ± 6 mg/kg, RTA 408 15 ± 4 mg/kg; p = 0.8) or duration of SE (vehicle 125±15 mins, RTA 408 130±10 mins; p = 0.5). For those that developed seizures, there was no significant difference in the latency period between SE and the first seizure for the two groups (median delay 13 days, interquartile range 7.25 days for vehicle treated animals; median delay 17.5 days, interquartile range 18 days for RTA 408 treated animals, p = 0.4 Mann-Whitney U test). In vehicle treated animals, the seizure frequency increased up to about 9 weeks (after first spontaneous seizure) and then plateaued. Although there was no significant difference in seizure frequency over the first 2 weeks between those animals given RTA 408 or vehicle, thereafter the seizure frequency was significantly less in those treated with RTA 408 (Fig. 5c,d). From weeks 9-12, there was a 94% reduction in median seizure frequency (from 23 to 1 per week, $p < 0.01$). Those animals treated with RTA 408 spent 60-80% of days with no seizures compared to 10-30% of days with no seizure for those animals that received vehicle ($p < 0.05$, Fig. 5e,f). There was, however, no difference in the distribution of seizure durations between the two groups (Fig. 5g). One out of 9 animals in the vehicle treated group did not develop epilepsy. The odds ratio for not developing epilepsy for RTA 408 versus vehicle groups was 4 (95% confidence interval 0.3-49), but this did not reach significance.

## Discussion

We have thus shown that the cyclic cyanoenone RTA 408 activates Nrf2 through inhibition of Keap1. Using an *in vitro* model of persistent seizure-like activity, we demonstrate that RTA 408 can prevent mitochondrial depolarization, ROS production, oxidative stress and consequent neuronal death. We translated these findings to an *in vivo* model of prolonged seizure activity, in

which we show that RTA 408 increases glutathione levels, increases ATP to supranormal levels, and similarly neuroprotects. Importantly, we found that RTA 408 administration has a disease-modifying effect, dramatically modifying the later development of spontaneous seizures.

Nrf2 is primarily negatively regulated by Kelch-like ECH associated protein 1 (Keap1)(Itoh *et al.*, 1999). Dimeric Keap1 sequesters Nrf2 in the cytoplasm and promotes degradation of Nrf2 through the ubiquitin-proteasome pathway(Cullinan *et al.*, 2004; Kobayashi *et al.*, 2004; Zhang *et al.*, 2004). Electrophiles and oxidants inactivate Keap1 by chemically modifying critical cysteine sensors within the protein(Dinkova-Kostova *et al.*, 2002), leading to Nrf2 accumulation and increased transcription of Nrf2 target genes(Baird and Dinkova-Kostova, 2011). The versatility and relatively long half-lives of the upregulated proteins ensure long-lasting protection against many different types of oxidants(Gao *et al.*, 2001). The cyclic cyanoenones are the most potent Nrf2 activators known to date(Dinkova-Kostova *et al.*, 2005; Honda *et al.*, 2011). The activated Michael acceptor functionality within their structures renders them highly reactive with sulfhydryl groups, and they belong to the category of drugs with reversible covalent mode of action, a property that makes them suitable for chronic administration(Kostov *et al.*, 2015). Although the mechanism of action of RTA 408 had been unclear, we show that it binds to C151 in Keap1, and so inhibits the interaction of Keap1 with Nrf2, enabling Nrf2 translocation to the nucleus(Cleasby *et al.*, 2014; Huerta *et al.*, 2016). In the nucleus, Nrf2 binds to the cis-acting antioxidant response elements (ARE), specific promoter sequences in genes encoding phase II and antioxidant cytoprotective proteins, including glutathione S-transferase, NADPH:quinone oxidoreductase (NQO1), and enzymes involved in the biosynthesis and regeneration of glutathione.

During prolonged seizures (SE), ROS are produced through activation of NADPH oxidase via NMDA receptor activation(Kovac *et al.*, 2014; Williams *et al.*, 2015). ROS and consequent peroxynitrite formation can contribute to cell death though lipid peroxidation, inactivation of enzymes, mitochondrial permeability transition pore opening (and mitochondrial depolarization) and DNA damage(Szabo *et al.*, 2007). Moreover, ROS can directly inhibit mitochondrial complex 1 activity, further impeding ATP production(Ryan *et al.*, 2012; Rowley *et al.*, 2015). Seizures and seizure-like activity are energy demanding processes with high ATP consumption by ion pumps; lower ATP production induced by ROS-induced mitochondrial dysfunction rapidly results in energy deprivation and cell death(Kovac *et al.*, 2012). In addition to increasing antioxidant cytoprotective proteins, overexpression or activation of Nrf2 can also suppress NADPH oxidase activity(Kovac *et al.*, 2015), and so should decrease ROS production and accumulation during seizure-like activity. We tested this in an *in vitro* model of seizure-like activity. Importantly, RTA 408 had no direct anti-seizure effect and did not alter the calcium dynamics of seizure-like activity, yet RTA 408 decreased ROS production, increased glutathione, restored ATP levels and neuroprotected. Thus the protective effect of RTA 408 can be explained by stimulation of mitochondrial bioenergetics and reduction of ROS production but not through inhibition of the calcium oscillations. However, these protective effects were observed in an *in vitro* model of prolonged seizure-like activity and caution has to be exercised in extrapolating this to the *in vivo* condition.

We, therefore, asked whether these *in vitro* results translate to an *in vivo* effect? To address this, we used an established *in vivo* model of SE, which results in neuronal death in the hippocampus in a similar pattern to that observed in human hippocampal sclerosis (the commonest cause of drug resistant epilepsy in humans)(Hellier *et al.*, 1998) and the development of chronic epilepsy.

In this model, RTA 408 administration over 3 days increased glutathione levels and rescued ATP decreases to supranormal levels by 1 week. This increase in antioxidants and cellular energy function resulted in neuroprotection in CA3 and the hilus. In this model, neuronal damage in CA1 was not evident until many weeks after the SE and since RTA 408 modified the development of epilepsy after 4 weeks, then it is unclear if the later neuroprotection in CA1 is a direct effect of RTA 408 or the result of decreasing the later seizure frequency. However, evidence in other models seems to indicate that the progression of damage after status epilepticus is not solely due to the occurrence of seizures(Pitkanen *et al.*, 2002), and it is also possible that the apparent progression that we observed could be due to such processes as the removal of dead or dying neurons. In addition, we (as others)(Gualtieri *et al.*, 2012) found evidence of loss of astrocytes with chemoconvulsant-induced status epilepticus; in our study, RTA 408 also effectively prevented this.

Acute RTA 408 administration reduced seizure frequency >8 weeks after the SE by > 90%. (at a time when RTA 408 would no longer be present) (SHEIKH, 2014). This compares very favourably to other disease modifying treatments. Although there was a tendency for there to be a greater number of seizure-free animals in the RTA 408 treated group, this did not reach significance. An unanswered question is whether longer administration could prevent the development of epilepsy altogether. Since the mechanism of action of RTA 408 is through modifying gene expression, it is noteworthy that it has a profound effect even when given after the epileptogenic insult, markedly increasing the translational potential of this intervention. RTA 408 is already undergoing clinical trials in other conditions, and the remarkable evidence of efficacy presented herein suggests potential for this drug as a disease-modifying treatment in epilepsy.

## Acknowledgments

We thank Dr. Andreas Lieb (UCL Institute of Neurology) for his assistance with the EEG analysis. The authors thank Reata Pharmaceuticals for their support and for providing RTA 408.

## Funding

This work was supported by the European Union's Seventh Framework Programme (FP7/2007-2013) under grant agreement n°602102 (EPITARGET) and Epilepsy Research UK and the Biotechnology and Biological Sciences Research Council (Project Grant BB/L01923X/1).

## References

Angelova PR, Abramov AY. Functional role of mitochondrial reactive oxygen species in physiology. Free Radic Biol Med 2016; 100: 81-5.

Baird L, Dinkova-Kostova AT. The cytoprotective role of the Keap1-Nrf2 pathway. Arch Toxicol 2011; 85(4): 241-72.

Ben-Ari Y. Limbic seizure and brain damage produced by kainic acid: mechanisms and relevance to human temporal lobe epilepsy. Neuroscience 1985; 14(2): 375-403.

Carrasco-Pozo C, Tan KN, Borges K. Sulforaphane is anticonvulsant and improves mitochondrial function. J Neurochem 2015; 135(5): 932-42.

Chang P, Hashemi KS, Walker MC. A novel telemetry system for recording EEG in small animals. J Neurosci Methods 2011; 201(1): 106-15.

Clarke JD, Hsu A, Williams DE, Dashwood RH, Stevens JF, Yamamoto M, et al. Metabolism and Tissue Distribution of Sulforaphane in Nrf2 Knockout and Wild-Type Mice. Pharm Res-Dordr 2011; 28(12): 3171-9.

Cleasby A, Yon J, Day PJ, Richardson C, Tickle IJ, Williams PA, et al. Structure of the BTB domain of Keap1 and its interaction with the triterpenoid antagonist CDDO. PLoS One 2014; 9(6): e98896.

Clulow JA, Storck EM, Lanyon-Hogg T, Kalesh KA, Jones LH, Tate EW. Competition-based, quantitative chemical proteomics in breast cancer cells identifies new target profiles for sulforaphane. Chem Commun (Camb) 2017; 53(37): 5182-5.

Cock HR, Tong X, Hargreaves IP, Heales SJ, Clark JB, Patsalos PN, et al. Mitochondrial dysfunction associated with neuronal death following status epilepticus in rat. Epilepsy Res 2002; 48(3): 157-68.

Copple IM, Shelton LM, Walsh J, Kratschmar DV, Lister A, Odermatt A, et al. Chemical tuning enhances both potency toward nrf2 and in vitro therapeutic index of triterpenoids. Toxicol Sci 2014; 140(2): 462-9.

Cullinan SB, Gordan JD, Jin J, Harper JW, Diehl JA. The Keap1-BTB protein is an adaptor that bridges Nrf2 to a Cul3-based E3 ligase: oxidative stress sensing by a Cul3-Keap1 ligase. Mol Cell Biol 2004; 24(19): 8477-86.

de Boer HM, Mula M, Sander JW. The global burden and stigma of epilepsy. Epilepsy Behav 2008; 12(4): 540-6.

Dinkova-Kostova AT, Abramov AY. The emerging role of Nrf2 in mitochondrial function. Free Radic Biol Med 2015; 88(Pt B): 179-88.

Dinkova-Kostova AT, Holtzclaw WD, Cole RN, Itoh K, Wakabayashi N, Katoh Y, et al. Direct evidence that sulfhydryl groups of Keap1 are the sensors regulating induction of phase 2 enzymes that protect against carcinogens and oxidants. Proc Natl Acad Sci U S A 2002; 99(18): 11908-13.

Dinkova-Kostova AT, Kostov RV, Canning P. Keap1, the cysteine-based mammalian intracellular sensor for electrophiles and oxidants. Arch Biochem Biophys 2017; 617: 84-93.

Dinkova-Kostova AT, Liby KT, Stephenson KK, Holtzclaw WD, Gao X, Suh N, et al. Extremely potent triterpenoid inducers of the phase 2 response: correlations of protection against oxidant and inflammatory stress. Proc Natl Acad Sci U S A 2005; 102(12): 4584-9.

Esteras N, Dinkova-Kostova AT, Abramov AY. Nrf2 activation in the treatment of neurodegenerative diseases: a focus on its role in mitochondrial bioenergetics and function. Biol Chem 2016; 397(5): 383-400.

Fahey JW, Dinkova-Kostova AT, Stephenson KK, Talalay P. The "Prochaska" microtiter plate bioassay for inducers of NQO1. Methods Enzymol 2004; 382: 243-58.

Galanopoulou AS, Buckmaster PS, Staley KJ, Moshe SL, Perucca E, Engel J, Jr., et al. Identification of new epilepsy treatments: issues in preclinical methodology. Epilepsia 2012; 53(3): 571-82.

Gao X, Dinkova-Kostova AT, Talalay P. Powerful and prolonged protection of human retinal pigment epithelial cells, keratinocytes, and mouse leukemia cells against oxidative damage: the indirect antioxidant effects of sulforaphane. Proc Natl Acad Sci U S A 2001; 98(26): 15221-6.

Gualtieri F, Curia G, Marinelli C, Biagini G. Increased perivascular laminin predicts damage to astrocytes in CA3 and piriform cortex following chemoconvulsive treatments. Neuroscience 2012; 218: 278-94.

Heinemann U, Kaufer D, Friedman A. Blood-brain barrier dysfunction, TGFbeta signaling, and astrocyte dysfunction in epilepsy. Glia 2012; 60(8): 1251-7.

Hellier JL, Patrylo PR, Buckmaster PS, Dudek FE. Recurrent spontaneous motor seizures after repeated low-dose systemic treatment with kainate: assessment of a rat model of temporal lobe epilepsy. Epilepsy Res 1998; 31(1): 73-84.

Higgins LG, Hayes JD. The cap'n'collar transcription factor Nrf2 mediates both intrinsic resistance to environmental stressors and an adaptive response elicited by chemopreventive agents that determines susceptibility to electrophilic xenobiotics. Chem Biol Interact 2011; 192(1-2): 37-45.

Holmstrom KM, Baird L, Zhang Y, Hargreaves I, Chalasani A, Land JM, et al. Nrf2 impacts cellular bioenergetics by controlling substrate availability for mitochondrial respiration. Biol Open 2013; 2(8): 761-70.

Honda T, Yoshizawa H, Sundararajan C, David E, Lajoie MJ, Favaloro FG, Jr., et al. Tricyclic compounds containing nonenolizable cyano enones. A novel class of highly potent anti-inflammatory and cytoprotective agents. J Med Chem 2011; 54(6): 1762-78.

Hopkins KJ, Wang G, Schmued LC. Temporal progression of kainic acid induced neuronal and myelin degeneration in the rat forebrain. Brain Res 2000; 864(1): 69-80.

Huerta C, Jiang X, Trevino I, Bender CF, Ferguson DA, Probst B, et al. Characterization of novel small-molecule NRF2 activators: Structural and biochemical validation of stereospecific KEAP1 binding. Biochim Biophys Acta 2016; 1860(11 Pt A): 2537-52.

Itoh K, Wakabayashi N, Katoh Y, Ishii T, Igarashi K, Engel JD, et al. Keap1 represses nuclear activation of antioxidant responsive elements by Nrf2 through binding to the amino-terminal Neh2 domain. Genes Dev 1999; 13(1): 76-86.

Jupp B, Williams J, Binns D, Hicks RJ, Cardamone L, Jones N, et al. Hypometabolism precedes limbic atrophy and spontaneous recurrent seizures in a rat model of TLE. Epilepsia 2012; 53(7): 1233-44.

Khalil A, Kovac S, Morris G, Walker MC. Carvacrol after status epilepticus (SE) prevents recurrent SE, early seizures, cell death, and cognitive decline. Epilepsia 2017; 58(2): 263-73.

Kim JH, Jang BG, Choi BY, Kim HS, Sohn M, Chung TN, et al. Post-treatment of an NADPH oxidase inhibitor prevents seizure-induced neuronal death. Brain Res 2013; 1499: 163-72.

Kobayashi A, Kang MI, Okawa H, Ohtsuji M, Zenke Y, Chiba T, et al. Oxidative stress sensor Keap1 functions as an adaptor for Cul3-based E3 ligase to regulate proteasomal degradation of Nrf2. Mol Cell Biol 2004; 24(16): 7130-9.

Kostov RV, Knatko EV, McLaughlin LA, Henderson CJ, Zheng S, Huang JT, et al. Pharmacokinetics and pharmacodynamics of orally administered acetylenic tricyclic bis(cyanoenone), a highly potent Nrf2 activator with a reversible covalent mode of action. Biochem Biophys Res Commun 2015; 465(3): 402-7.

Kovac S, Angelova PR, Holmstrom KM, Zhang Y, Dinkova-Kostova AT, Abramov AY. Nrf2 regulates ROS production by mitochondria and NADPH oxidase. Biochim Biophys Acta 2015; 1850(4): 794-801.

Kovac S, Domijan AM, Walker MC, Abramov AY. Prolonged seizure activity impairs mitochondrial bioenergetics and induces cell death. J Cell Sci 2012; 125(Pt 7): 1796-806.

Kovac S, Domijan AM, Walker MC, Abramov AY. Seizure activity results in calcium- and mitochondria-independent ROS production via NADPH and xanthine oxidase activation. Cell Death Dis 2014; 5: e1442.

Liu SJ, Zheng P, Wright DK, Dezsi G, Braine E, Nguyen T, et al. Sodium selenate retards epileptogenesis in acquired epilepsy models reversing changes in protein phosphatase 2A and hyperphosphorylated tau. Brain 2016; 139(Pt 7): 1919-38.

Hayens LW. H. The Neuron in Tissue Culture. New York, NY, USA: Wiley; 1999.

Mazzuferi M, Kumar G, van Eyll J, Danis B, Foerch P, Kaminski RM. Nrf2 defense pathway: Experimental evidence for its protective role in epilepsy. Ann Neurol 2013; 74(4): 560-8.

Pauletti A, Terrone G, Shekh-Ahmad T, Salamone A, Ravizza T, Rizzi M, et al. Targeting oxidative stress improves disease outcomes in a rat model of acquired epilepsy. Brain 2017.

Paxinos G. WC. The Rat Brain in Stereotaxic Coordinates. 4th ed. San Diego: Academic Press; 1998.

Pitkanen A, Lukasiuk K. Mechanisms of epileptogenesis and potential treatment targets. Lancet Neurol 2011; 10(2): 173-86.

Pitkanen A, Nissinen J, Nairismagi J, Lukasiuk K, Grohn OH, Miettinen R, et al. Progression of neuronal damage after status epilepticus and during spontaneous seizures in a rat model of temporal lobe epilepsy. Prog Brain Res 2002; 135: 67-83.

Racine RJ. Modification of seizure activity by electrical stimulation. II. Motor seizure. Electroencephalogr Clin Neurophysiol 1972; 32(3): 281-94.

Reschke CR, Henshall DC. microRNA and Epilepsy. Adv Exp Med Biol 2015; 888: 41-70.

Rowley S, Liang LP, Fulton R, Shimizu T, Day B, Patel M. Mitochondrial respiration deficits driven by reactive oxygen species in experimental temporal lobe epilepsy. Neurobiol Dis 2015; 75: 151-8.

Ryan K, Backos DS, Reigan P, Patel M. Post-translational oxidative modification and inactivation of mitochondrial complex I in epileptogenesis. J Neurosci 2012; 32(33): 11250-8.

Saito R, Suzuki T, Hiramoto K, Asami S, Naganuma E, Suda H, et al. Characterizations of Three Major Cysteine Sensors of Keap1 in Stress Response. Mol Cell Biol 2015; 36(2): 271-84.

Schuchmann S, Buchheim K, Meierkord H, Heinemann U. A relative energy failure is associated with low-Mg2+ but not with 4-aminopyridine induced seizure-like events in entorhinal cortex. J Neurophysiol 1999; 81(1): 399-403.

SHEIKH AYPS, Deerfield, Illinois, 60015, US), MATTEI, Alessandra (130 S. Canal Street, Apt. 701Chicago, Illinois, 60606, US), WANG, Xiu C. (1649 Saddle Hill Road, Green Oaks, Illinois, 60048, US), inventor ABBVIE INC. (1 North Waukegan Road, North Chicago, Illinois, 60064, US), assignee. 2,2-DIFLUOROPROPIONAMIDE DERIVATIVES OF BARDOXOLONE METHYL, POLYMORPHIC FORMS AND METHODS OF USE THEREOF. 2014.

Socala K, Nieoczym D, Kowalczuk-Vasilev E, Wyska E, Wlaz P. Increased seizure susceptibility and other toxicity symptoms following acute sulforaphane treatment in mice. Toxicol Appl Pharmacol 2017; 326: 43-53.

Szabo C, Ischiropoulos H, Radi R. Peroxynitrite: biochemistry, pathophysiology and development of therapeutics. Nat Rev Drug Discov 2007; 6(8): 662-80.

Vezzani A, French J, Bartfai T, Baram TZ. The role of inflammation in epilepsy. Nat Rev Neurol 2011; 7(1): 31-40.

Walsh J, Jenkins RE, Wong M, Olayanju A, Powell H, Copple I, et al. Identification and quantification of the basal and inducible Nrf2-dependent proteomes in mouse liver: biochemical, pharmacological and toxicological implications. J Proteomics 2014; 108: 171-87.

Wang W, Wang WP, Zhang GL, Wu YF, Xie T, Kan MC, et al. Activation of Nrf2-ARE signal pathway in hippocampus of amygdala kindling rats. Neurosci Lett 2013; 543: 58-63.

Williams PA, White AM, Clark S, Ferraro DJ, Swiercz W, Staley KJ, et al. Development of spontaneous recurrent seizures after kainate-induced status epilepticus. J Neurosci 2009; 29(7): 2103-12.

Williams S, Hamil N, Abramov AY, Walker MC, Kovac S. Status epilepticus results in persistent overproduction of reactive oxygen species, inhibition of which is neuroprotective. Neuroscience 2015; 303: 160-5.

Zhang DD, Lo SC, Cross JV, Templeton DJ, Hannink M. Keap1 is a redox-regulated substrate adaptor protein for a Cul3-dependent ubiquitin ligase complex. Mol Cell Biol 2004; 24(24): 10941-53.

## Figure legends

**Figure 1. RTA 408 increases Nrf2 through inhibition of KEAP1.** (a) Chemical structure of RTA 408. (b, c) Induction of NQO1 by RTA 408 in Hepa1c1c7 cells (b), and wild-type (WT)and Nrf2-knockout MEF cells (c). Cells ($10^4$ per well) were grown for 24 h in 96-well plates, and subsequently exposed to RTA 408 for 48 h (b) or 24 h (c). There were eight replicates of each treatment of eight inducer concentrations. At the end of the treatment period, cell lysates were prepared in digitonin and the specific activity of NQO1 was determined using menadione as a substrate. Mean values for the eight replicate wells are shown. The standard deviation for each data point was within 5% of the value. (d, e) Western blot analyses of total cell lysates of Keap1-knockout MEF cells rescued with either WT, single cysteine mutant C151S, double cysteine mutant C273W/C288E, or triple cysteine mutant C151S/C273W/C288E of mouse N-terminally tagged HA-Keap1 (d) or primary peritoneal macrophages isolated from WT or Keap1$^{C151S/C151S}$ knock-in mice (e). Cells grown for 24 h in 6-well plates were exposed to vehicle (0.1% DMSO) or RTA 408 for a further 3 h, after which the cells were lysed. Immunoblotting was performed on whole cell lysates using antibodies against Nrf2, HA, Keap1 and α-tubulin.

**Figure 2. RTA 408 decreases ROS production, and prevents mitochondrial membrane depolarization and neuronal death during seizure-like activity in cortical neurons.**

Synchronous $Ca^{2+}$ oscillatory indicates seizure-like activity in neurons induced by replacement of aCSF with low-$Mg^{2+}$ aCSF in control (a, n = 70 neurons, 1 experiment (exp.)) and in RTA 408 (200 nM, 24 h) treated culture (b, n = 72 neurons, 1 exp.). RTA 408 changed neither the

frequency (c, $t(11) = 1.644$, $p = 0.129$, n = 627 neurons from 7 exp. for low Mg2+; n = 536 neurons from 6 exp. for RTA 408 (200 nM, 24 h)) nor the coastline (d, $t(11) = 2.245$, $p=0.811$) of $Ca^{2+}$ oscillations. (e) Left panel: Representative traces of mitochondrial membrane potential ($\Delta\psi m$) in neurons (mean ± SEM) in aCSF (black line; n=112 neurons, 1 exp.), low-$Mg^{2+}$ (red; n=120 neurons, 1 exp.) and neurons exposed to low magnesium preincubated with RTA 408 (200 nM) for 24 h (blue; n=106 neurons, 1 exp.). FCCP (1 μM; set to 100%) was added to cultures at the end of each experiment. Arrow indicates replacement of aCSF with low-$Mg^{2+}$ aCSF. Right panel: bar chart showing normalized Rhodamine123 fluorescence of neurons in aCSF (n = 559 neurons, n=6 exp.) during low-$Mg^{2+}$ treatment (n=627 neurons, 7 exp), RTA 408 preincubated cultures with 50 nM for 24 h (n = 410 neurons, 5 exp.) and for 48 h (n = 416 neurons, 5 exp.) and with 200nM for 24 h (n = 536 neurons, 6 exp.), at different time points following exposure low-$Mg^{2+}$. (f) Left panel: Representative experiments of neuronal HEt fluorescence measurements in aCSF (black, n=91 neurons, 1 exp.), low-$Mg^{2+}$ condition (red line, n=88 neurons, 1 CS), and in neurons exposed to low-$Mg^{2+}$ preincubated with RTA 408 (200 nM, 24 h) (blue line, n = 96 neurons, 1 exp.). Right panel: bar chart summarizing the rates (mean ± SEM) of ROS production at 2, 10 and 15 minutes in aCSF (n = 353 neurons, 4 exp.), after omission of $Mg^{2+}$ from the extracellular solution (low-$Mg^{2+}$; n =4 03 neurons, 5 exp.,) and RTA 408 treated neurons in low-$Mg^{2+}$ condition (n = 496 neurons, 6 exp.). (e-f) Data were analyzed by repeated measures one-way ANOVA (e: $F(4,24) = 26.689$, $p < 0.001$; f: $F(2,12) = 49.415$, $p < 0.001$) followed by Bonferroni post hoc tests. $^{**}p < 0.01$, $^{***}$ $p< 0.001$ relative to low-$Mg^{2+}$ condition. (g) Low-$Mg^{2+}$ (n = 9 exp.) treatment significantly decreases the level of GSH (measured using MCB fluorescence) compared to aCSF (n = 10 exp.) and RTA 408 (200 nM, 24 h) pretreated cultures (n = 10 exp.). (h) Percentage of dead neurons in cultures exposed to low-

$Mg^{2+}$ (n = 9 exp.) is significantly higher when compared with exposure to aCSF (2 h; n = 9 exp.) and RTA 408 (200 nM, 24 h) preincubated cultures exposed to low-$Mg^{2+}$ (2 h; n=9 exp.). (g-h) Data were analyzed by one-way ANOVA (g: $F(2,26) = 12.425$, $p < 0.001$; h: $F(2,24) = 22.100$, $p < 0.001$) with Bonferroni post hoc test $^{**}p < 0.01$, $^{***}p < 0.001$ relative to low-$Mg^{2+}$ condition.

**Figure 3. RTA 408 rescues total glutathione (GSH) and ATP levels following KA-induces SE *in vivo*.** (a) Total (oxidized and reduced forms of GSH) were measured in the cortex and hippocampus of sham rats (Sham; n = 7 for cortex and n = 6 for hippocampus), and from treated rats 7 days following KA-induced SE (2 h), followed by vehicle (10% DMSO/Saline KA + vehicle; n = 5), RTA 408 groups at doses: 17.5 mg/kg once daily for 3 days (KA + RTA 17.5; n = 6), 25mg/kg once daily for 3 days (KA + RTA 25; n = 5) and 50mg/kg once daily for 2 days (KA + RTA 50; n = 6). (b) ATP levels measured in the same animals (Sham; n = 6), vehicle (KA + vehicle; n = 5), RTA 408 17.5 mg/kg once daily for 3 days (KA + RTA 17.5; n = 5), RTA 408 25 mg/kg once daily for 3 days (KA + RTA 25; n = 5) and RTA 408 50 mg/kg once daily for 2 days (KA + RTA 50; n= 6).

Data are expressed as mean±SEM. $^{*}p < 0.05$, $^{**}p < 0.01$ and $^{***}p < 0.001$ versus KA group, by one-way ANOVA with Bonferroni *post hoc* test. In a, cortex: $F(4,24) = 18.197$, $p < 0.001$; Hippocampus : $F(4,22) = 101.409$, $p < 0.001$; In b, cortex: $F(4,21) = 11.738$, $p < 0.001$; Hippocampus: $F(4,21) = 20.262$, $p < 0.001$.

**Figure 4. RTA 408 prevents neuronal cell death following KA-induced SE in rats.** (a) Representative images for CA1, CA3 and hilus of coronal sections from vehicle (10% DMSO/Saline) treated and RTA 408 treated rats 15 weeks after SE; scale bar = 100 μM. (b-g)

Cell densities in CA1, CA3 and hilus of sham (n=6), and vehicle (n = 5) and RTA 408 (25 mg/kg/day for 3 days; n = 5) treated rats 1 week (b-d) and 15 weeks (e-g); in sham (n = 6), vehicle (n = 7), RTA 408 (25 mg/kg/day for 1 day; n = 5) and RTA 408 (25 mg/kg/day for 3 days; n = 7) following 2 h KA induced SE. Data are expressed as mean ± SEM numbers of animals. *$p < 0.05$, **$p < 0.01$ and ***$p < 0.001$ compared to vehicle group by one-way ANOVA followed by Bonferroni *post hoc* test. b: $F(2,13) = 2.806$, $p = 0.097$; c: $F(2,13) = 9.220$, $p = 0.003$; d: $F(2,13) = 42.138$, $p < 0.001$; e: $F(2,13) = 20.536$, $p < 0.001$; f: $F(2,13) = 10.236$, $p < 0.001$; g: $F(2,13) = 24.550$, $p < 0.001$.

**Figure 5. RTA 408 modifies seizure progression.** (a) EEG sample traces recorded for status epilepticus (SE): An asterisk indicates the beginning of SE whereas an arrow indicates termination with Diazepam. (b) Typical EEG example of a spontaneous seizure post SE, expanded in the right panel. Note the rhythmical high frequency discharges at the beginning of the seizure (2) when compared to baseline (1). This rhythmic fast activity increases in amplitude (3) and decreases in frequency (4) towards the end of the seizure thus fulfilling the criteria for EEG seizure activity. (c-d) Bar charts of mean frequency (± SEM) of electrographically recorded seizures following KA induced SE for control rats, treated with vehicle (10% DMSO/Saline) once daily for 3 days (n = 9) and RTA 408 treated rats (RTA 408 25 mg/kg once daily for 3 days; n = 9) 1-12 weeks (c; $F(1,192) = 5.828$, $p < 0.05$) and 13-15 weeks following the first spontaneous seizure (d; $F(1,18) = 10.163$, $p < 0.01$); Animal numbers in d: n = 4 for both groups. * $p < 0.05$, ** $p < 0.01$ and *** $p < 0.001$ by generalized log-linear mixed model followed by sequential Bonferroni post hoc test. (e) Probability distribution illustrating the probability of 0-10

seizures/day for each individual vehicle (n = 9) and RTA 408 treated rat (n = 9). (f) Bar chart summarizing mean ± SEM seizure probability across time ** $p < 0.01$ probabilities of seizure free days were compared using Mann-Whitney U. (g) Seizure duration distribution for the same animals as in panel c, demonstrating no significant difference between vehicle or RTA408 treated animals.

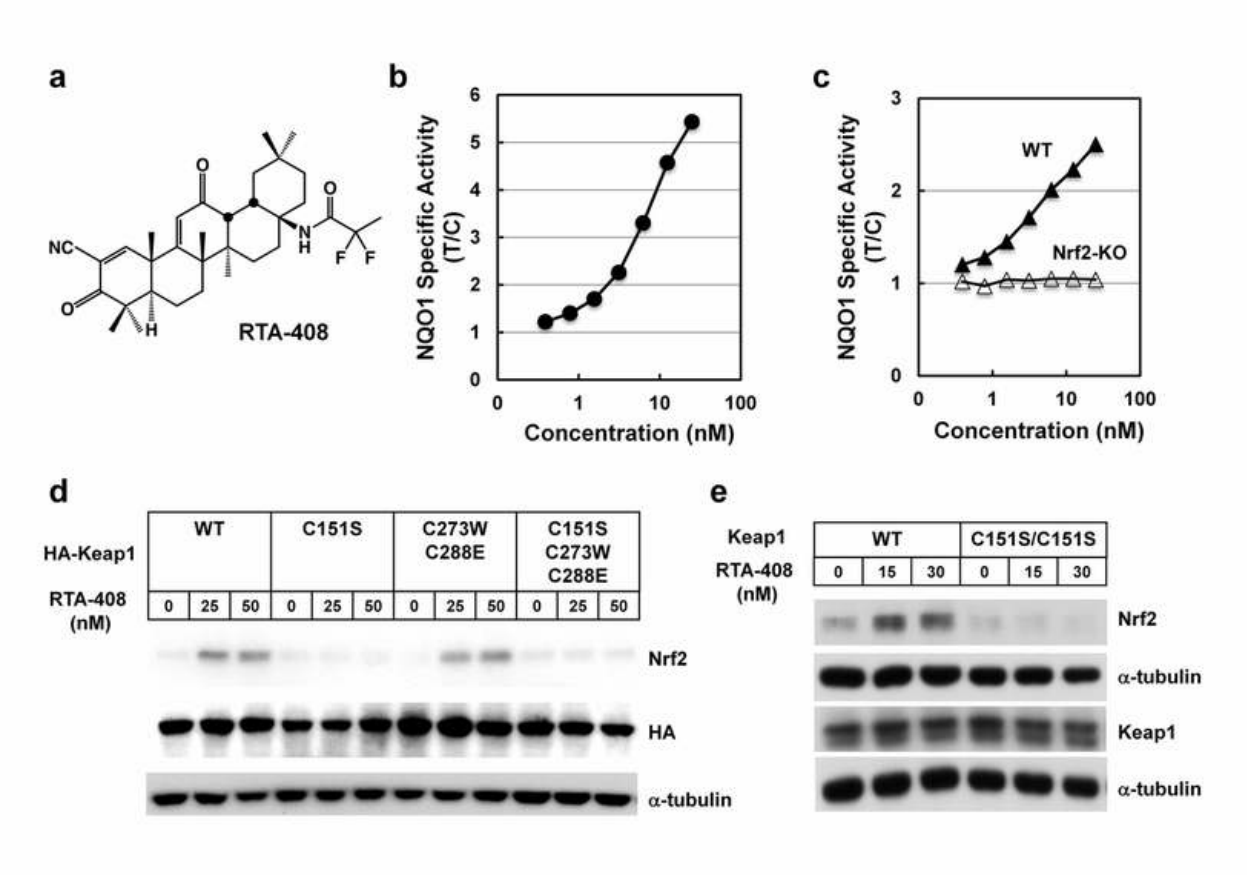
a
RTA-408
b
NQO1 Specific Activity (T/C)
Concentration (nM)
c
WT
Nrf2-KO
NQO1 Specific Activity (T/C)
Concentration (nM)
d
HA-Keap1
WT
C151S
C273W C288E
C151S C273W C288E
RTA-408 (nM)
0 25 50 0 25 50 0 25 50 0 25 50
Nrf2
HA
α-tubulin
e
Keap1
WT
C151S/C151S
RTA-408 (nM)
0 15 30 0 15 30
Nrf2
α-tubulin
Keap1
α-tubulin

Figure 1

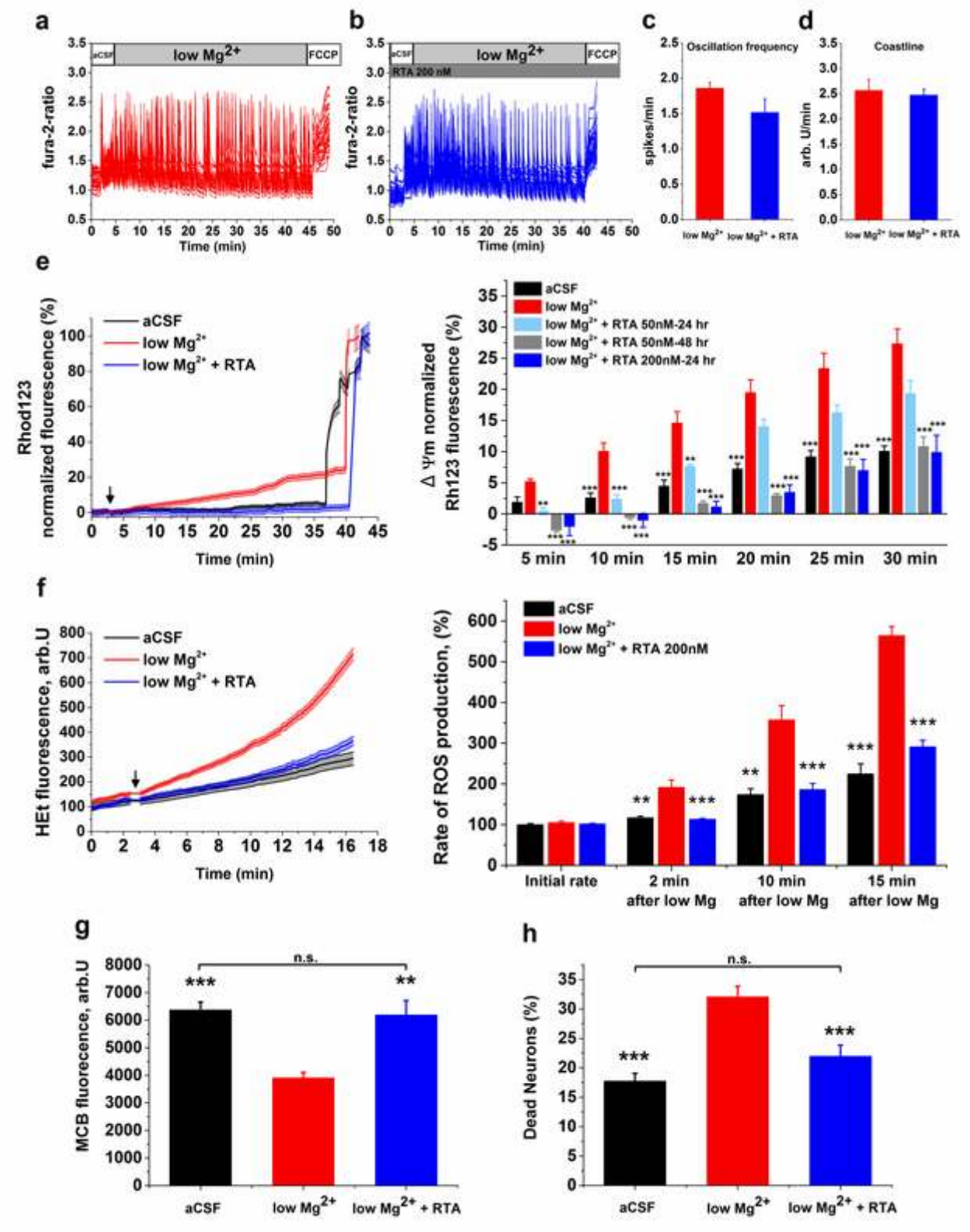
a
b
c
d
aCSF
low Mg2+
FCCP
RTA 200 nM
fura-2-ratio
Time (min)
Oscillation frequency
spikes/min
Coastline
arb. U/min
low Mg2+
low Mg2+ + RTA
e
Rhod123
normalized flourescence (%)
aCSF
low Mg2+
low Mg2+ + RTA
Δ Ψm normalized
Rh123 fluorescence (%)
low Mg2+ + RTA 50nM-24 hr
low Mg2+ + RTA 50nM-48 hr
low Mg2+ + RTA 200nM-24 hr
5 min
10 min
15 min
20 min
25 min
30 min
f
HEt fluorescence, arb.U
Rate of ROS production, (%)
low Mg2+ + RTA 200nM
Initial rate
2 min
after low Mg
10 min
after low Mg
15 min
after low Mg
g
MCB fluorecence, arb.U
n.s.
h
Dead Neurons (%)

Figure 2

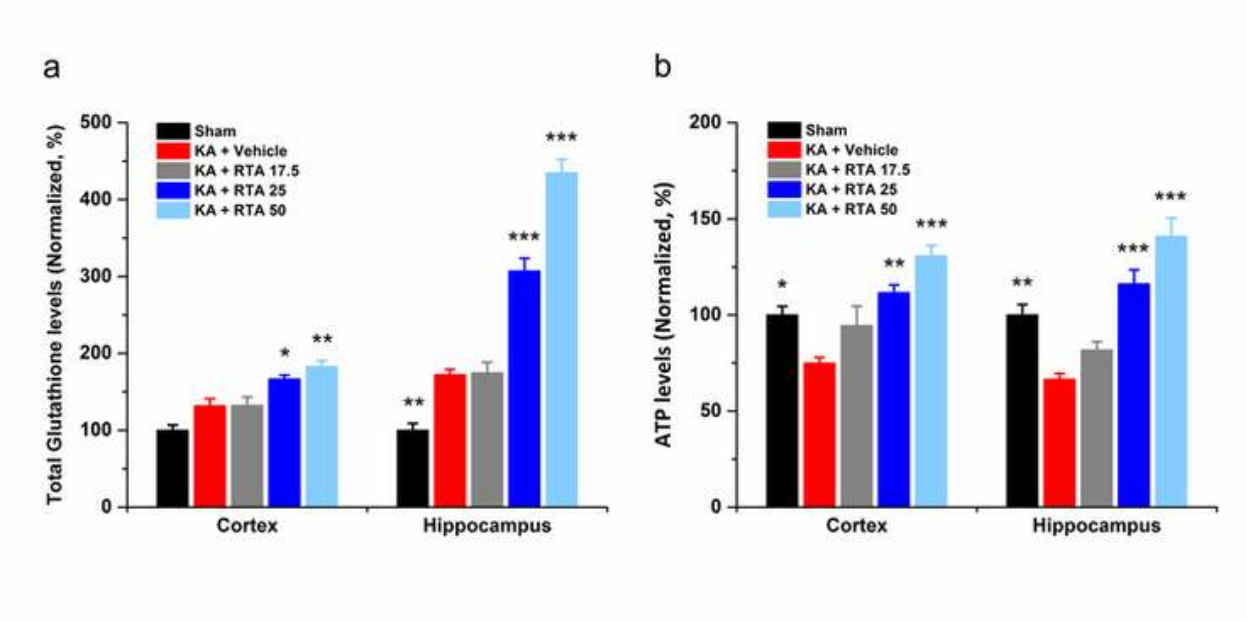
a
Total Glutathione levels (Normalized, %)
500
400
300
200
100
0
Sham
KA + Vehicle
KA + RTA 17.5
KA + RTA 25
KA + RTA 50
*
**
**
***
***
Cortex
Hippocampus
b
ATP levels (Normalized, %)
200
150
100
50
0
Sham
KA + Vehicle
KA + RTA 17.5
KA + RTA 25
KA + RTA 50
*
**
***
**
***
***
Cortex
Hippocampus

Figure 3

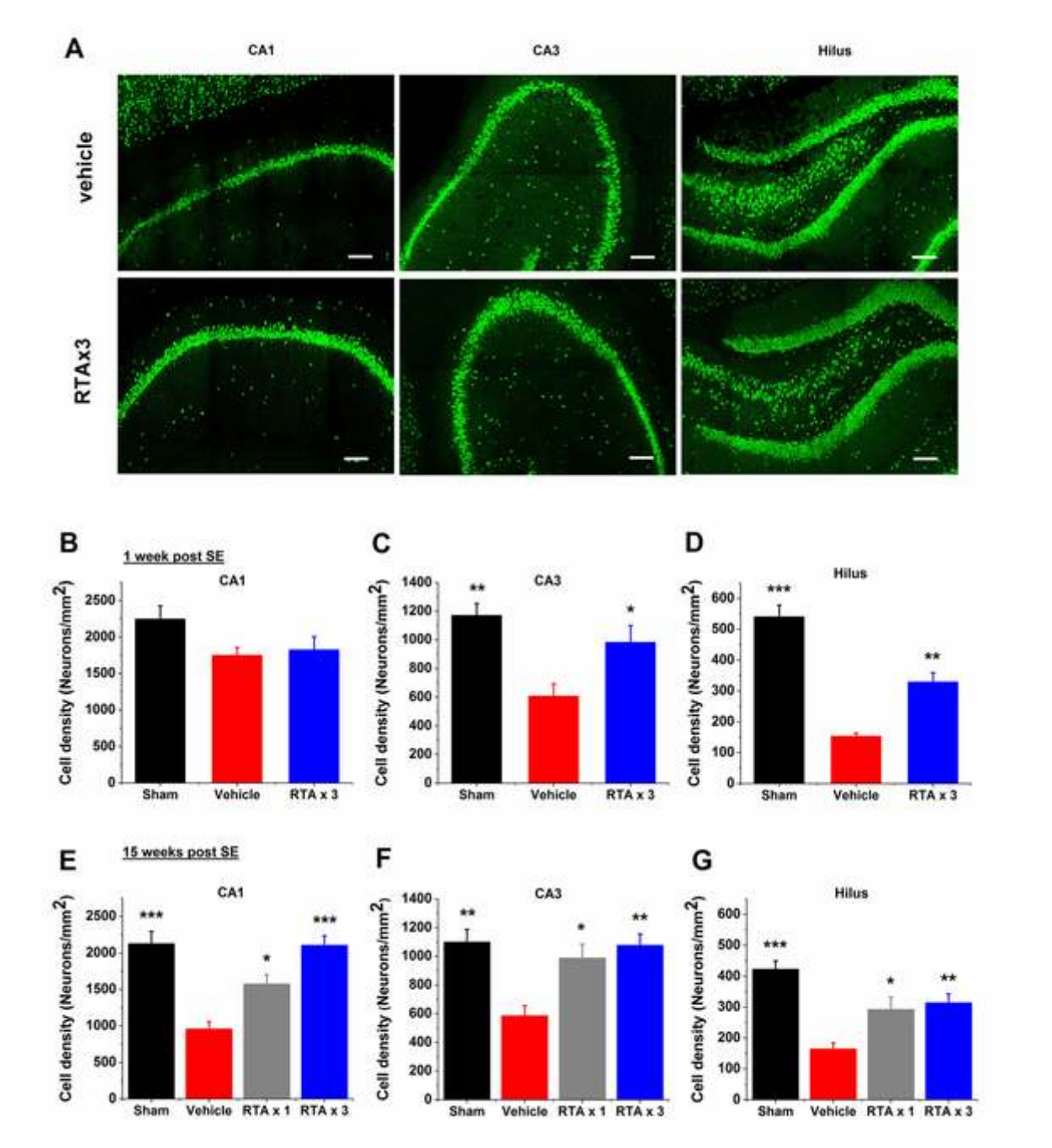
A
CA1
CA3
Hilus
vehicle
RTAx3
B
1 week post SE
CA1
Cell density (Neurons/mm2)
Sham
Vehicle
RTA x 3
C
CA3
D
Hilus
E
15 weeks post SE
RTA x 1
F
G

Figure 4

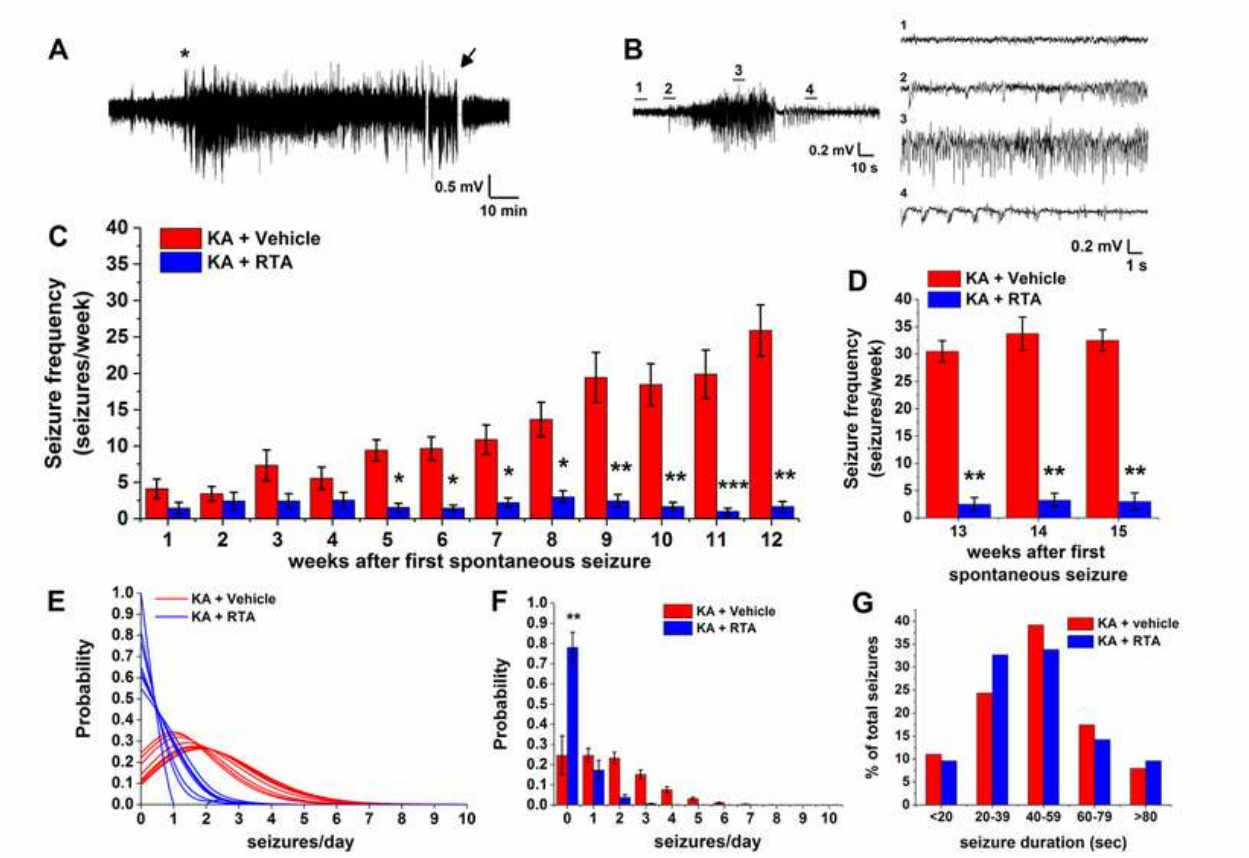
A
B
C
D
E
F
G
0.5 mV
10 min
0.2 mV
10 s
0.2 mV
1 s
KA + Vehicle
KA + RTA
Seizure frequency (seizures/week)
weeks after first spontaneous seizure
Probability
seizures/day
% of total seizures
seizure duration (sec)
<20
20-39
40-59
60-79
>80

Figure 5

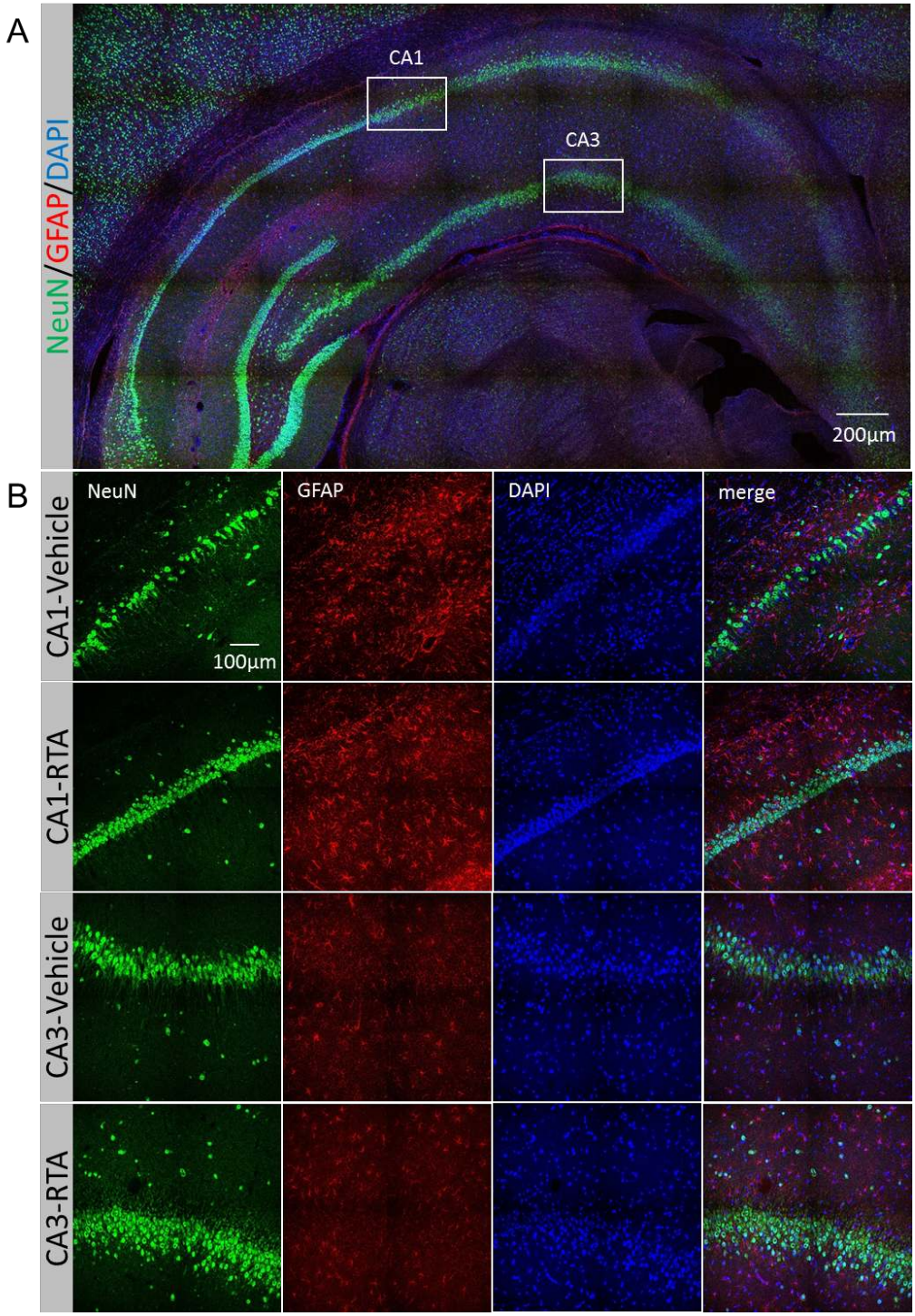


**Supplementary Figure 1.** Immunohistochemical analyses of the rat ventral hippocampus 15 weeks after SE. (A) Coronal section of the rat ventral hippocampus immunostained for a neuronal marker (NeuN), the astrocytic marker glial fibrillary acidic protein (GFAP) and DAPI in RTA 408 treated rat. (B) Representative images for immunostaining in the CA1 and CA3 regions of the hippocampus of rats treated with vehicle or RTA 408 (25 mg/kg) for 3 days after KA induced SE.

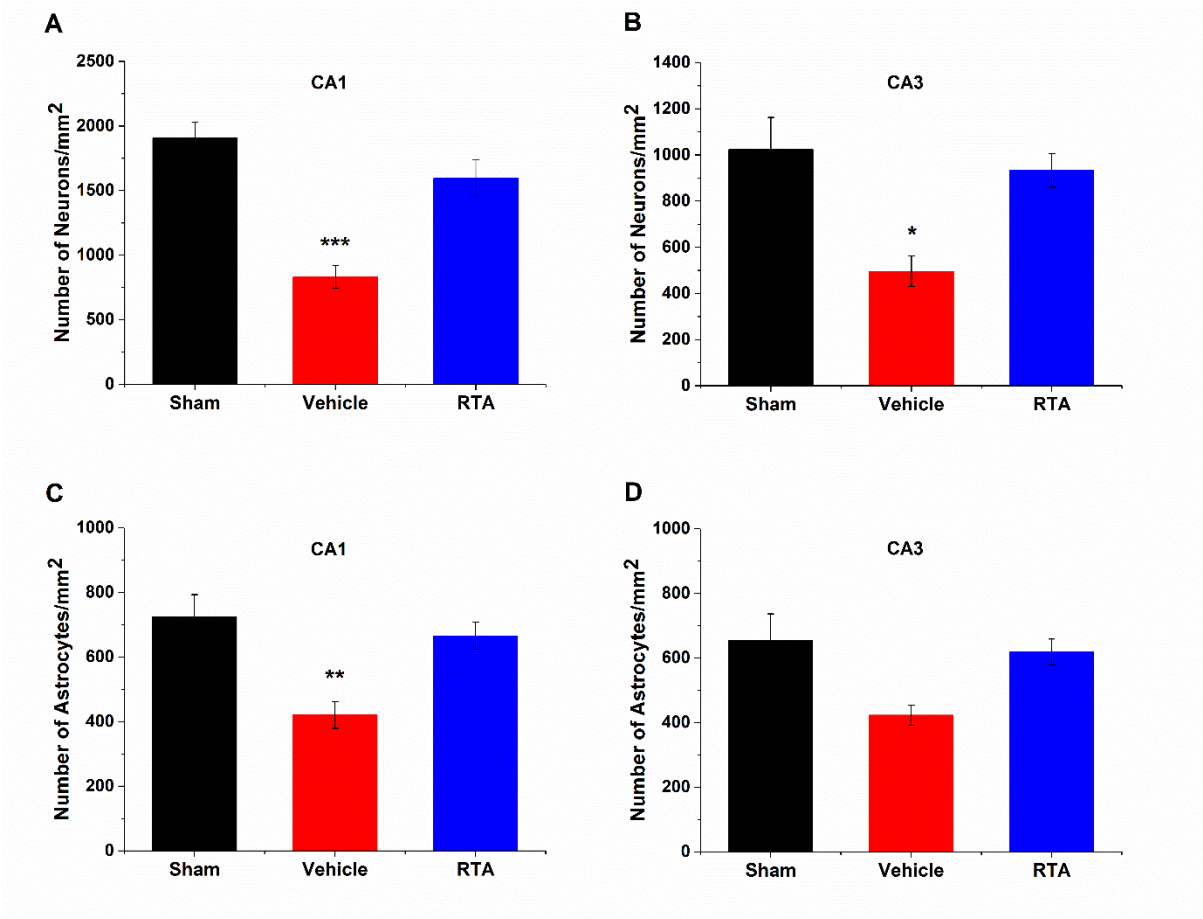


**Supplementary Figure 2.** Neuronal and astrocytic cell densities in CA1 and CA3 of the rat ventral hippocampus 15 weeks after SE. Neuronal cell densities in CA1 (A) and CA3 (B) and astrocytic cell density of CA1 (C) and CA3 (D) (of the same areas analysed in A and B, respectively) of sham (black, n=5), and vehicle (red, n=5) and RTA 408 (25 mg/kg/day for 3 days; blue, n = 5) treated rats 15 week following 2 h KA induced SE. Data are expressed as mean±SEM. *$p < 0.05$, **$p < 0.01$ and ***$p < 0.001$ compared to sham group by one-way ANOVA followed by Tukey's post hoc test.